

# THE PHYSICAL REVIEW

*A journal of experimental and theoretical physics established by E. L. Nichols in 1893*

SECOND SERIES, VOL. 64, NOS. 9 AND 10

NOVEMBER 1 AND 15, 1943

## Rotational Analysis of the Emission Spectrum of CuF

L. H. WOODS

*Ryerson Physical Laboratories, University of Chicago, Chicago, Illinois*

(Received August 21, 1943)

The emission spectrum of gaseous HF at pressures of about 0.1 mm in a copper hollow cathode has been examined from 7000 to 2000A and an unknown band spectrum of widely spaced lines lying in the region 2450–2600A thought to be the  ${}^2\Sigma \rightarrow {}^2\Pi$  transition of HF<sup>+</sup> has been found. From the same source the emission spectrum of CuF has been obtained and was photographed on the 30,000-lines-per-inch Chicago grating spectrograph. The spectrum consists of 3 band systems lying at 5700A, 5060A, and 4920A. A rotational analysis of the spectrum has shown the three systems to have the same lower state, and to be of the type  ${}^1\Pi \rightarrow {}^1\Sigma$ ,  ${}^1\Sigma \rightarrow {}^1\Sigma$ , and  ${}^1\Pi \rightarrow {}^1\Sigma$ . The constants of these states are given in the following table:

| State          | Transition        | $\nu_0$   | $B_0$ cm <sup>-1</sup> | $D_0$ cm <sup>-1</sup> | $r_0$ (A) | $\nu_1$  | $B_1$  | $r_1$ |
|----------------|-------------------|-----------|------------------------|------------------------|-----------|----------|--------|-------|
| C ${}^1\Pi$    | C $\rightarrow$ X | 20,269.62 | 0.3748                 | $5.06 \times 10^{-7}$  | 1.755     |          |        |       |
| B ${}^1\Sigma$ | B $\rightarrow$ X | 19,734.66 | 0.3700                 | $4.8 \times 10^{-7}$   | 1.769     | 19769.92 | 0.3650 | 1.779 |
| A ${}^1\Pi$    | A $\rightarrow$ X | 17,556.40 | 0.3675                 |                        | 1.773     |          |        |       |
| X ${}^1\Sigma$ |                   |           | 0.3780                 | $5.6 \times 10^{-7}$   | 1.749     |          | 0.3734 | 1.759 |

The calculated rotational isotope effect has been found to check very well that measured experimentally.

### I. INTRODUCTION

THE emission spectrum of CuF was first described by Mulliken,<sup>1</sup> who obtained very weak exposures of the bands by heating CuF<sub>2</sub> in active nitrogen. He inferred that the bands obtained from CuF<sub>2</sub> are emitted by the diatomic molecule CuF, on the basis that (1) the bands of other copper halides are excited from either cupric or cuprous salts, and (2) the vibrational analysis and isotope effects of the bands of the other copper halides indicate them to belong to the diatomic molecules CuX. The vibrational analysis of the absorption spectrum of CuF was published by Ritschl<sup>2</sup> in 1927. He photographed the spectrum from vapor at 2000°C on a seven

meter grating, obtaining resolution of the vibrational but not the rotational structure. The spectrum consists of three band systems, whose rotational structure is degraded to the red and whose vibrational structure is degraded to the violet, lying at 5700A, 5060A, 4920A, with increasing intensity in this order, and respectively referred to as A, B, and C. Using the frequencies of the band heads, Ritschl was able to make a vibrational analysis which showed that the B and C systems had the same lower state, and he assumed the A system also to have, an hypothesis supported by the conclusions reached in this paper.

The present study of the CuF bands is a by-product of a search for the emission spectrum of HF, which has been sought unsuccessfully in the past by many experimenters. In the present ex-

<sup>1</sup> R. S. Mulliken, Phys. Rev. **26**, 1 (1925).

<sup>2</sup> R. Ritschl, Zeits. f. Physik **42**, 172 (1927).

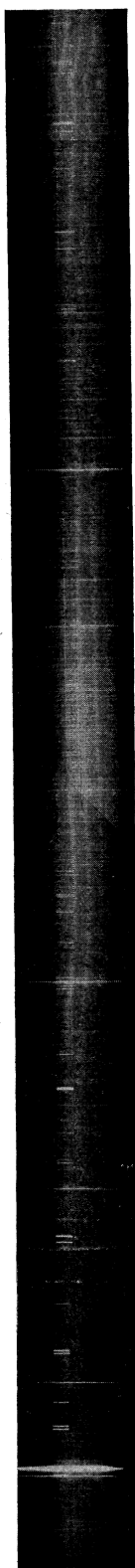


FIG. 1. The group of lines around 2500Å of the  ${}^2\Pi \rightarrow {}^2\Sigma$  system of  $\text{HF}^+$ .

periments there has been obtained an unknown spectrum with very widely spaced lines, such as would be emitted by a diatomic hydride molecule. This is thought to belong to  $\text{HF}^+$ . It lies in the region 2450Å–2600Å, which agrees well with the position predicted from the location of the known  $\text{HCl}^+$  and  $\text{HBr}^+$   ${}^2\Sigma \rightarrow {}^2\Pi$  spectra. The identification is not complete, however, because the spectrum has not been analyzed.

In looking for possible bands of HF, the spectral region from 2000Å to 6600Å was examined, and in this way were obtained the present photographs of the  $\text{CuF}$  band system. In these, both the rotational structure and rotational isotope splitting were resolved and the following rotational analysis was made. Previously, the nature of some of the electronic states of  $\text{CuCl}$  had been deduced by Terrien<sup>3</sup> from the appearance of the emission spectrum. He identified a  ${}^1\Sigma$  ground state and a  ${}^1\Pi$  and a  ${}^1\Sigma$  excited state.

## II. EXPERIMENTAL

The spectra were obtained from a small water-cooled hollow cathode made of copper, through which flowed gaseous HF at pressures of about 0.1 mm of mercury. The cathode was run from a 2000 volt d.c. generator at a current of about 0.3 ampere. The

<sup>3</sup> Jean Terrien, Theses, University of Paris, 1937.

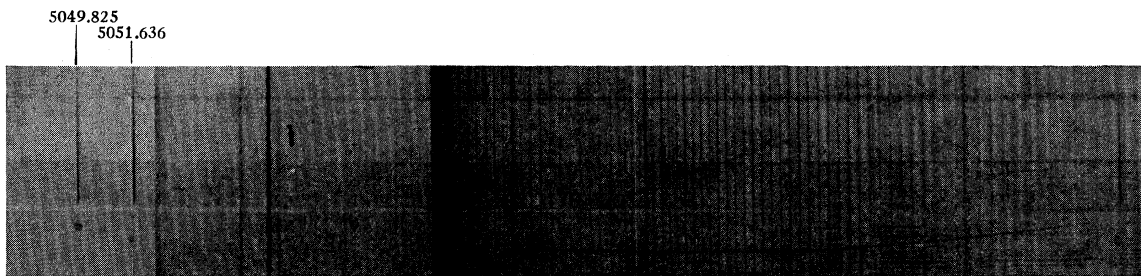
anode was insulated from the cathode by a thick glass ring, and the edges where copper met glass were sealed with Apiezon Q wax. The design of the cathode is very like that used by Mrozowski<sup>4</sup> for the  $\text{HgH}^+$  and  $\text{HgD}^+$  spectra with the exception that (1) there is no long glass sleeve running far down between anode and cathode, (2) the gas is introduced into the cathode through an opening at the end, and (3) the window opening is small. This last condition was necessary because the window of the discharge tube was a small flat crystal of artificial white sapphire ( $\text{Al}_2\text{O}_3$ ; alundum) about  $1 \times 1\frac{1}{2}$  mm in size. Its valuable properties, described by Freed, McMurry, and Rosenbaum,<sup>5</sup> are enthusiastically supported by these experiments. After several hundred hours of contact with flowing anhydrous HF gas, although it has been cleaned several times of sputtered copper, the crystal is as clear as glass and shows no corrosion. Its transmitting properties seem equally as good as those of quartz to 2000Å, so far as these experiments could detect.

The HF was generated in a copper oven, a tube about  $1\frac{1}{2}$ " in diameter and 16" long, by decomposition of anhydrous  $\text{KHF}_2$  at about 275°C according to the equation  $\text{KHF}_2 \rightarrow \text{KF} + \text{HF}$ . The lower end of the oven was closed with a screwed-in plug of copper and sealed with silver solder. At the upper end, the lid and delivery tube which led to the cathode were sealed with soft solder to facilitate recharging with fresh  $\text{KHF}_2$ . To prevent this seal from softening when the oven was heated, the seal was water-cooled with a copper coil. The HF gas flowed through the delivery tube, through the cathode, passed through a copper to glass seal, and was condensed in two successive glass traps at liquid nitrogen temperatures. After an exposure the traps were removed and washed with large quantities of water to dissolve and dilute the liquid HF (boiling point = 19.5°C). The traps prevented the HF from flowing into the oil and mercury pumps, which were run continuously during the long exposures to prevent accumulation of impurities.

The group of lines around 2500Å believed to belong to  $\text{HF}^+$  (Fig. 1) was excited only in the

<sup>4</sup> S. Mrozowski, Phys. Rev. **58**, 332 (1940).

<sup>5</sup> Freed, McMurry, and Rosenbaum, J. Chem. Phys. **7**, 853 (1939).

FIG. 2. An enlargement of the (0'-0) and (1-1) bands of the  ${}^1\Sigma \rightarrow {}^1\Sigma$  system at 5060A.

flowing gas. Under these conditions the discharge was deep red with a bluish cast. In stagnant gas the bands of CO, CO<sub>2</sub>, and SiF became very strong, the color of the discharge turned blue, and the 2500A band disappeared presumably because the pressure increased and the electrons were slower. The glass ring which insulated the anode from the cathode provided a constant source of SiF, but this impurity was not present in large

amounts in the flowing gas. The CuF bands were excited even in the stagnant gas discharge; however under these conditions their analysis was interfered with by many overlapping bands of impurities. The CuF bands were obtained quite free from foreign spectra when excited in the flowing gas. Presence of helium did not increase the intensity of the bands.

By use of a slit width of 20 microns, the *B* and *C* bands were photographed on Eastman 144-B plates in the first order of the 30-foot Chicago grating. Photographs of these bands in the higher orders could not be obtained because the second and third orders at 5000A are too weak. Unfortunately the *A* system at 5700A, which is the least intense of the three, fell on the position of the slit, and it was necessary to photograph this band with an older grating which has about one-third the intensity of the new grating. In order to obtain a picture, it was therefore imperative to photograph this band system on Eastman 103-D plates, with a wide slit and a current of 1.6 amperes, but even under these conditions, the photograph obtained, although adequate, is not impressive, and the analysis of this band has consequently suffered.

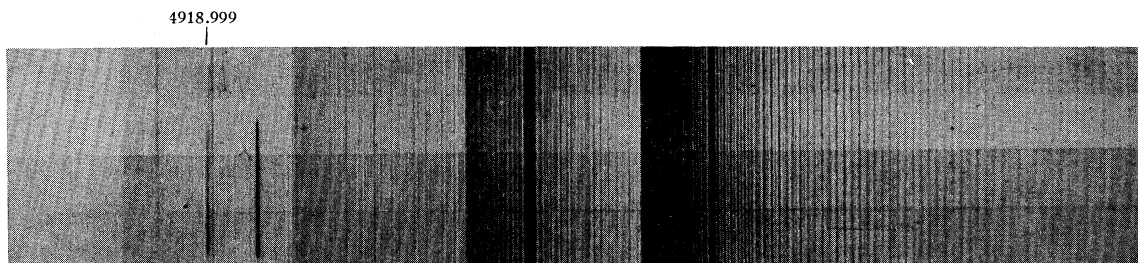
### III. ANALYSIS

#### *B* System

The *B* system at 5060A is a  $v' = v''$  vibrational sequence of bands of the type  ${}^1\Sigma \rightarrow {}^1\Sigma$  (Fig. 2). Although Ritschl observed both  $v' = v''$  and  $v'' + 1 = v'$  sequences in absorption, only the  $v' = v''$  sequence appeared in the emission spectrum. Even after a 56-hour exposure, the  $v' = v'' + 1$  sequence did not appear on the plates. The zero gap is clearly visible.  $P(J) - P(J-1)$  and  $R(J) - R(J-1)$  were plotted along the same

TABLE I.  ${}^1\Sigma \rightarrow {}^1\Sigma$  transition of CuF [0→0].  $\nu_0 = 19,734.66$ .

| <i>J</i> | <i>P</i> | <i>R</i> | <i>P<sub>i</sub></i> | <i>J</i> | <i>P</i> | <i>R</i>   | <i>P<sub>i</sub></i> |
|----------|----------|----------|----------------------|----------|----------|------------|----------------------|
| 0        | —        | —        | —                    | 41       | 19691.01 | —          | 10691.20             |
| 1        | 19733.89 | 19736.01 | —                    | 42       | 89.65    | —          | 89.88                |
| 2        | 3.12     | 6.88     | —                    | 43       | 8.25     | —          | 8.48                 |
| 3        | 2.36     | 7.62     | —                    | 44       | 6.80     | —          | 7.09                 |
| 4        | 1.60     | 8.25     | —                    | 45       | 5.42     | —          | 5.69                 |
| 5        | 0.80     | 8.87     | —                    | 46       | 19684.03 | —          | 19684.26             |
| 6        | 19729.91 | 19739.48 | —                    | 47       | 2.59     | —          | 2.80                 |
| 7        | 9.09     | 40.11    | —                    | 48       | 1.11     | —          | 1.80                 |
| 8        | 8.22     | 0.72     | —                    | 49       | 79.66    | —          | 79.96                |
| 9        | 7.28     | 1.37     | —                    | 50       | 8.17     | —          | 8.42                 |
| 10       | 6.41     | 1.98     | —                    | 51       | 19676.70 | 19752.50bh | 19677.01             |
| 11       | 19725.52 | 19742.55 | —                    | 52       | 5.23     | —          | 5.55                 |
| 12       | 4.60     | 3.09     | —                    | 53       | 3.68     | —          | 4.03                 |
| 13       | 3.67     | 3.60     | —                    | 54       | 2.15     | —          | 2.51                 |
| 14       | 2.70     | 4.10     | —                    | 55       | 0.62     | —          | 0.98                 |
| 15       | 1.73     | 4.61     | —                    | 56       | 19669.05 | —          | 19669.43             |
| 16       | 19720.71 | 19745.10 | —                    | 57       | 7.53     | —          | 7.86                 |
| 17       | 19.69    | 5.60     | —                    | 58       | 5.95     | —          | 6.31                 |
| 18       | 8.66     | 6.04     | —                    | 59       | 4.36     | —          | 4.79                 |
| 19       | 7.65     | 6.46     | —                    | 60       | 2.77     | —          | 3.16                 |
| 20       | 6.61     | 6.87     | —                    | 61       | 19661.18 | —          | 19661.59             |
| 21       | 19715.55 | 19747.27 | —                    | 62       | 59.54    | —          | 0.02                 |
| 22       | 4.45     | 7.66     | —                    | 63       | 7.97     | 19750.53   | 58.39                |
| 23       | 3.34     | 8.04     | —                    | 64       | 6.27     | —          | 6.75                 |
| 24       | 2.22     | 8.40     | —                    | 65       | 4.65     | —          | 5.11                 |
| 25       | 1.09     | 8.76     | —                    | 66       | 19652.98 | 19749.73   | 19653.45             |
| 26       | 19709.96 | 19749.08 | —                    | 67       | 1.29     | —          | 1.80                 |
| 27       | 8.93     | 49.40    | —                    | 68       | 49.64    | —          | 0.15                 |
| 28       | 7.62     | 9.73     | —                    | 69       | 7.96     | —          | 8.76                 |
| 29       | 6.41     | 50.02    | —                    | 70       | 6.24     | —          | 8.39                 |
| 30       | 5.23     | 0.28     | —                    | 71       | 19644.51 | 19748.04   | 19645.06             |
| 31       | 19704.00 | 19750.53 | —                    | 72       | 2.83     | —          | 3.33                 |
| 32       | 2.75     | —        | —                    | 73       | 1.13     | —          | 1.73                 |
| 33       | 1.48     | —        | —                    | 74       | 39.32    | —          | 6.87                 |
| 34       | 0.23     | —        | —                    | 75       | 7.48     | —          | 6.46                 |
| 35       | 698.92   | —        | 19699.14             | 76       | 19635.93 | 19746.04   | —                    |
| 36       | 19697.60 | —        | 19697.84             | 77       | 4.18     | —          | 5.60                 |
| 37       | 6.36     | —        | 6.56                 | 78       | 2.42     | —          | 5.10                 |
| 38       | 5.03     | —        | 5.27                 | 79       | 0.55     | —          | 4.61                 |
| 39       | 3.75     | —        | 3.99                 | 80       | 28.81    | —          | 4.10                 |
| 40       | 2.36     | —        | 2.63                 | 81       | 19626.65 | 19743.80   | —                    |
|          |          |          |                      | 82       | 5.18     | —          | 3.09                 |

Fig. 3. An enlargement of the  $C$  system ( ${}^1\Pi\rightarrow{}^1\Sigma$ ) at 4920A.

line against  $J$ . From the slope of this line, which is equal to  $2(B_0' - B_0'')$ , was obtained the value  $B_0' - B_0'' = -0.00805 \text{ cm}^{-1}$ . The  $J$  numbering given here (Table I), which classifies the three unobserved central lines as the true missing line, the  $R(0)$  line, and the  $P(1)$  line, was assumed correct, with the reservation that it may err by one unit because of the faintness of  $P$  and  $R$  lines of low  $J$  values. From plots of the  $\Delta_2 F$  values based on this numbering, the values  $B_0'' = 0.3780 \pm 0.0005 \text{ cm}^{-1}$  and  $B_0' = 0.3700 \pm 0.0005 \text{ cm}^{-1}$  were obtained. These figures are consistent with the value for  $(B_0' - B_0'')$ . The value of  $B_0''$  is corroborated by the analysis of system  $C$ . For this reason the  $J$  numbering as given here is believed to be correct. The only possible alternative  $J$  numbering, namely that which increases the  $J$  value of each  $R$  line and decreases that of each  $P$  line by one unit, gives values  $B_0'' = 0.3850 \text{ cm}^{-1}$  and  $B_0' = 0.3770 \text{ cm}^{-1}$ . From the theoretical relation  $D_v = 4B_v^3/\omega_v^2$ , and Ritschl's  $\omega_v$  values,  $D_0' = 4.8 \times 10^{-7}$  and  $D_0'' = 5.6 \times 10^{-7} \text{ cm}^{-1}$  were calculated. The slopes of the curves  $[R(J-1) - P(J+1)]/(4J+2)$  and  $[R(J) - P(J)]/(4J+2)$  plotted against  $J^2$  gave the approximate values  $D_0' = 10 \times 10^{-7} \text{ cm}^{-1}$  and  $D_0'' = 11 \times 10^{-7} \text{ cm}^{-1}$ .

### C System

The  $C$  system at 4920A is a  $v' = v''$  vibrational sequence of bands (Table II) of the type  ${}^1\Pi\rightarrow{}^1\Sigma$  (Fig. 3). The intense band heads are  $Q$  branches, the strong edge of each band being the origin of the  $Q$  branch. The  $P$  branch of the  $0\rightarrow 0$  band is easily traced toward decreasing wave-lengths until it becomes too faint to be seen, but the  $R$  branch, which starts with low intensity from the origin, runs through the  $1\rightarrow 1$   $P$  branch into the intense  $1\rightarrow 1$   $Q$  branch overlapped by  $2\rightarrow 2$   $P$  and  $Q$  branches. It cannot be traced through this

thicket of lines. At approximately  $J=74$  where the intensity is no longer large, it is calculated to reach a head which cannot be seen because it is covered by the intense  $1\rightarrow 1$   $Q$  head. The slopes of the two lines  $P(J) - P(J-1)$  and  $Q(J) - Q(J-1)$  plotted against  $J$  gave the values  $B_0'(P) - B_0'' = -0.0027 \text{ cm}^{-1}$  and  $B_0'(Q) - B_0'' = -0.0037 \text{ cm}^{-1}$ .

TABLE II.  ${}^1\Pi\rightarrow{}^1\Sigma$  transition of  $\text{CuF}$  ( $0\rightarrow 0$ ).  $\nu_0 = 20,269.62 \text{ cm}^{-1}$ .

| $J$ | $P(\text{cm}^{-1})$ | $Q(\text{cm}^{-1})$ | $P_i(\text{cm}^{-1})$ | $J$ | $P(\text{cm}^{-1})$ | $Q(\text{cm}^{-1})$ | $P_i(\text{cm}^{-1})$ |
|-----|---------------------|---------------------|-----------------------|-----|---------------------|---------------------|-----------------------|
| 8   | 20263.05            | —                   | —                     | 51  | 20224.05            | 20258.58            | 20224.32              |
| 9   | 2.37                | —                   | —                     | 52  | 3.04                | 8.21                | 3.33                  |
| 10  | 1.65                | —                   | —                     | 53  | 2.02                | 7.72                | 2.27                  |
|     |                     |                     |                       | 54  | 0.97                | 7.36                | 1.25                  |
| 11  | 20260.96            | —                   | —                     | 55  | 219.91              | 6.87                | 0.17                  |
| 12  | 0.21                | —                   | —                     |     |                     |                     |                       |
| 13  | 59.41               | —                   | —                     | 56  | 20218.86            | 20256.48            | 20219.21              |
| 14  | 8.61                | —                   | —                     | 57  | 7.88                | 5.99                | 8.15                  |
| 15  | 7.73                | —                   | —                     | 58  | 6.77                | 5.53                | 7.13                  |
|     |                     |                     |                       | 59  | 5.76                | 5.01                | 6.03                  |
| 16  | 20256.88            | —                   | —                     | 60  | 4.72                | 4.61                | 4.96                  |
| 17  | 6.07                | —                   | —                     |     |                     |                     |                       |
| 18  | 5.22                | 20268.29            | —                     | 61  | 20213.57            | 20254.05            | 20213.93              |
| 19  | 4.36                | 8.07                | —                     | 62  | 2.52                | 3.60                | 2.86                  |
| 20  | 3.53                | 7.89                | —                     | 63  | 1.41                | 3.09                | 1.88                  |
|     |                     |                     |                       | 64  | 0.44                | 2.66                | 0.73                  |
| 21  | 20252.63            | 20267.67            | —                     | 65  | 09.36               | 2.08                | 09.65                 |
| 22  | 1.80                | 7.50                | —                     |     |                     |                     |                       |
| 23  | 0.90                | 7.35                | —                     | 66  | 20208.24            | 20251.63            | 20208.68              |
| 24  | 49.99               | 7.10                | —                     | 67  | 7.21                | 1.10                | 7.49                  |
| 25  | 9.10                | 6.90                | —                     | 68  | 6.10                | 0.64                | 6.41                  |
|     |                     |                     |                       | 69  | 4.96                | 0.04                | 5.30                  |
| 26  | 20248.17            | 20266.65            | —                     | 70  | 3.88                | 49.63               | 4.21                  |
| 27  | 7.28                | 6.45                | —                     |     |                     |                     |                       |
| 28  | 6.37                | 6.18                | —                     | 71  | 20202.76            | 20248.98            | 20203.14              |
| 29  | 5.49                | 5.99                | —                     | 72  | 1.65                | 8.79                | 2.07                  |
| 30  | 4.56                | 5.71                | —                     | 73  | 0.62                | 7.88                | 0.95                  |
|     |                     |                     |                       | 74  | 199.50              | 7.31                | 199.84                |
| 31  | 20243.58            | 20265.45            | —                     | 75  | 8.39                | 6.77                | 8.73                  |
| 32  | 2.64                | 5.14                | —                     |     |                     |                     |                       |
| 33  | 1.75                | 4.91                | —                     | 76  | 20196.86            | 20246.22            | 20197.71              |
| 34  | 0.80                | 4.54                | —                     | 77  | 6.21                | 5.67                | —                     |
| 35  | 39.83               | 4.34                | —                     | 78  | 5.09                | 5.04                | —                     |
|     |                     |                     |                       | 79  | 3.98                | 4.50                | —                     |
| 36  | 20238.91            | 20263.96            | —                     | 80  | 2.85                | 4.33                | 3.22                  |
| 37  | 7.93                | 3.70                | —                     |     |                     |                     |                       |
| 38  | 7.00                | 3.37                | —                     | 81  | 20191.73            | 20243.31            | 20192.01              |
| 39  | 6.00                | 3.11                | —                     | 82  | 0.62                | 2.70                | 0.90                  |
| 40  | 5.05                | 2.66                | —                     | 83  | 89.43               | 2.17                | 89.82                 |
|     |                     |                     |                       | 84  | 8.31                | 1.51                | —                     |
| 41  | 20234.05            | 20262.43            | —                     | 85  | 7.23                | 0.93                | —                     |
| 42  | 3.08                | 1.99                | —                     |     |                     |                     |                       |
| 43  | 2.09                | 1.77                | —                     | 86  | 20186.10            | 20240.28            | —                     |
| 44  | 1.11                | 1.29                | —                     | 87  | 4.98                | 39.59               | —                     |
| 45  | 0.12                | 1.00                | —                     | 88  | 3.80                | —                   | —                     |
|     |                     |                     |                       | 89  | 2.56                | 8.48                | —                     |
| 46  | 20229.17            | 20260.51            | —                     |     |                     |                     |                       |
| 47  | 8.13                | 0.20                | —                     |     |                     |                     |                       |
| 48  | 7.09                | 59.72               | 20227.31              |     |                     |                     |                       |
| 49  | 6.08                | 9.36                | 6.40                  |     |                     |                     |                       |
| 50  | 5.07                | 8.95                | 5.30                  |     |                     |                     |                       |

Because it was impossible to measure the  $R$  branch, the exact  $\Delta_2 F^o$ 's for the lower state could not be obtained independently. But the quantity  $Q(J) - Q(J-1) - P(J) - P(J+1)$ , which is equal to the  $\Delta_2 F(J)$  for the lower state plus the quantum defect of the  ${}^1\Pi$  state, was plotted against  $J$  for several possible  $J$  numberings of the  $Q$  and  $P$  branches. The slopes of the curves were computed at low  $J$  values, where the possible error due to the quantum defect was small, and compared with the slopes of the  $\Delta_2 F$  curves obtained for the two possible  $J$  numberings of the 5060A band. In one and only one way of numbering was it

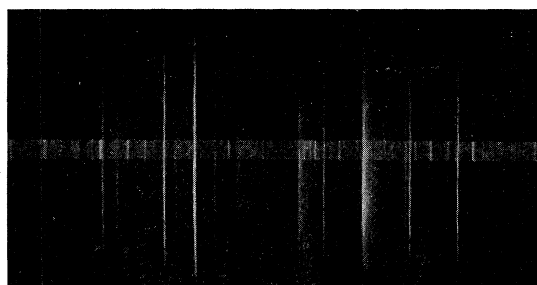


FIG. 4. The  $A$  system of CuF at 5690A of the type  ${}^1\Pi \rightarrow {}^1\Sigma$ .

TABLE III.  ${}^1\Pi \rightarrow {}^1\Sigma$  transition of CuF ( $0 \rightarrow 0$ ). Band head at 17556.40.

| $J$ | $P(\text{cm}^{-1})$ | $P_i(\text{cm}^{-1})$ | $J$ | $P(\text{cm}^{-1})$ | $P_i(\text{cm}^{-1})$ |
|-----|---------------------|-----------------------|-----|---------------------|-----------------------|
| 1   |                     |                       | 41  | 17509.06            | 17509.44              |
| 2   | 17555.08            | —                     | 42  | 7.57                | 7.96                  |
| 3   | 4.30                |                       | 43  | 6.08                | 6.50                  |
| 4   | 3.43                |                       | 44  | 4.62                | 4.97                  |
| 5   | 2.49                |                       | 45  | 3.08                | 3.48                  |
| 6   | 17551.59            | —                     | 46  | 17501.55            | 17502.03              |
| 7   | 0.68                |                       | 47  | 0.02                | 0.53                  |
| 8   | 49.73               |                       | 48  | 498.54              | 498.97                |
| 9   | 8.81                |                       | 49  | 6.96                | 7.45                  |
| 10  | 7.88                |                       | 50  | 5.32                | 5.84                  |
| 11  | 17546.94            | —                     | 51  | 17493.91            | 17494.31              |
| 12  | 5.91                |                       | 52  | 2.30                | 2.81                  |
| 13  | 4.88                |                       | 53  | 0.76                | 1.17                  |
| 14  | 3.83                |                       | 54  | 89.13               | 89.65                 |
| 15  | 2.80                |                       | 55  | 7.60                | 8.11                  |
| 16  | 17541.70            | —                     | 56  | 17486.98            | 17486.44              |
| 17  | 0.54                |                       | 57  | 4.40                | 4.91                  |
| 18  | 39.46               |                       | 58  | 2.77                | 3.26                  |
| 19  | 8.36                |                       | 59  | 1.14                | 1.71                  |
| 20  | 7.16                |                       | 60  | 79.51               | —                     |
| 21  | 17535.96            | —                     | 61  | 17477.91            | 17478.41              |
| 22  | 4.79                |                       | 62  | 6.28                | 6.77                  |
| 23  | 3.53                |                       | 63  | 4.69                | 4.97                  |
| 24  | 2.33                |                       | 64  | 3.00                | —                     |
| 25  | 1.07                |                       | 65  | 1.44                | —                     |
| 26  | 17529.79            | —                     | 66  | 17469.75            | —                     |
| 27  | 8.52                |                       | 67  | 8.06                | —                     |
| 28  | 7.16                |                       | 68  | 6.40                | —                     |
| 29  | 5.86                |                       | 69  | 4.74                | —                     |
| 30  | 4.52                |                       | 70  | 3.09                | —                     |
| 31  | 17523.22            | —                     | 71  | 17461.42            | —                     |
| 32  | 1.85                |                       | 72  | 59.73               | —                     |
| 33  | 0.51                |                       | 73  | 8.14                | —                     |
| 34  | 19.08               |                       | 74  | 6.39                | —                     |
| 35  | 7.72                |                       | 75  | 4.71                | —                     |
| 36  | 17516.36            | —                     | 76  | 17453.05            | —                     |
| 37  | 4.86                |                       | 77  | —                   | —                     |
| 38  | 3.39                |                       |     |                     |                       |
| 39  | 1.97                |                       |     |                     |                       |
| 40  | 0.53                | 17511.00              |     |                     |                       |

possible to get equal slopes for the curves of the two bands, indicating that the  $J$  numberings which they represented gave the same  $B_0''$  for the lower states of transitions  $C$  and  $B$ , and the  $J$  numberings thus found are those given here.  $\{Q(J) + Q(J+1) - P(J) - P(J+1)\}/(4J+2)$ , plotted against  $J$  and extrapolated to  $J=0$  gave  $B_0'(Q) = 0.373 \text{ cm}^{-1}$ .  $\{Q(J) + Q(J-1) - P(J) - P(J-1)\}/(4J+2)$  similarly treated gave  $B_0'' = 0.3775 \text{ cm}^{-1}$ , in agreement with the value of  $B_0''$  obtained from the analysis of the 5060A  ${}^1\Sigma \rightarrow {}^1\Sigma$  band. One concludes from this value that the two transitions have the same lower state, confirming the results of Ritschl's vibrational analysis. The lower state must be a  ${}^1\Sigma$  state. There are two upper states, a  ${}^1\Pi$  and a  ${}^1\Sigma$ , whose separation is  $534.96 \text{ cm}^{-1}$ .

From the quantities  $B_0'(P) - B_0'' = -0.0027$ ,  $B_0'(Q) - B_0'' = -0.0037$ , and  $B_0'' = 0.3775 \text{ cm}^{-1}$ , the values  $B_0'(P) = 0.3748$  and  $B_0'(Q) = 0.3738 \text{ cm}^{-1}$  are readily obtained. Unfortunately,  $B_0'(Q)$  differs somewhat from the value obtained by extrapolation given above.

Kronig<sup>6</sup> and Van Vleck<sup>7</sup> have shown that the splitting of the rotational levels caused by the interaction of rotation and electronic motion may be expressed by a term of the form  $qJ(J+1)$  where  $q = B_0'(P) - B_0'(Q)$ . In this case the experimental value of  $q$ , the difference of the  $B$ 's, is  $0.0010 \text{ cm}^{-1}$ . For the case of Van Vleck's pure precession between a  ${}^1\Pi$  and a  ${}^1\Sigma$  state, the theoretical value of  $q$  is given by  $q = 2B_0^2 l(l+1)/\nu(\Pi, \Sigma)$ , which in this case has the value  $0.0011 \text{ cm}^{-1}$ . The experimental value  $0.0010 \text{ cm}^{-1}$  was tested in the following equation  $P(J+1) - Q(J) + 2B_0''(J+1) + 2D_0''(J+1)^2 = qJ(J+1)$  over a

<sup>6</sup> R. de L. Kronig, *Zeits. f. Physik* **50**, 347 (1928).

<sup>7</sup> J. H. Van Vleck, *Phys. Rev.* **37**, 733 (1929).

TABLE IV.  ${}^1\Sigma \rightarrow {}^1\Sigma$  transition of CuF (1 $\rightarrow$ 1).

| $J$ | $R(\text{cm}^{-1})$ | $P(\text{cm}^{-1})$ | $J$ | $R(\text{cm}^{-1})$ | $P(\text{cm}^{-1})$ |
|-----|---------------------|---------------------|-----|---------------------|---------------------|
| 0   | —                   | —                   | 16  | 19780.30            | 19756.09            |
| 1   | 19771.75            | —                   | 17  | 0.79                | 5.11                |
| 2   | 2.47                | —                   | 18  | 1.23                | 4.15                |
| 3   | 3.19                | 19768.11            | 19  | 1.61                | 3.06                |
| 4   | 3.81                | 6.72                | 20  | 1.99                | —                   |
| 5   | 4.42                | 6.01                | 21  | 19782.37            | —                   |
| 6   | 19775.05            | 19765.13            | 22  | 2.74                | —                   |
| 7   | 5.79                | 4.26                | 23  | 3.12                | —                   |
| 8   | 6.20                | 3.47                | 24  | 3.45                | —                   |
| 9   | 6.79                | 2.56                | 25  | 3.72                | —                   |
| 10  | 7.29                | 1.71                | 26  | 19784.08            | —                   |
| 11  | 19777.87            | 19760.77            | 27  | 4.36                | —                   |
| 12  | 8.39                | 59.90               | 28  | 4.67                | —                   |
| 13  | 8.87                | 8.90                |     |                     |                     |
| 14  | 9.36                | 7.97                |     |                     |                     |
| 15  | 9.84                | 7.08                |     |                     |                     |

range of 80 units of  $J$  with satisfactory results. The values  $D_0' = 5.06 \times 10^{-7}$  and  $D_0'' = 5.60 \times 10^{-7}$  were calculated from the equations  $D_0' = 4B_0'^3/\omega_0^2$  and  $D_0'' = 4B_0''^3/\omega_0^2$ , where  $B = \frac{1}{2}B(P) + \frac{1}{2}B(Q)$ .

### A System

Band *A* at 5690A (Table III) is also of the type  ${}^1\Pi \rightarrow {}^1\Sigma$  (Fig. 4). The band edges are heads of  $Q$  branches, but unfortunately the  $Q$  lines cannot be measured. At low  $J$  values they merge into the gray background which forms the head, and at high  $J$  values they are too faint. The  $R$  branch, lost in the overlapping lines of the 1 $\rightarrow$ 1 and 2 $\rightarrow$ 2 transitions, cannot be measured either. The slope of the curve  $P(J) - P(J-1)$  plotted against  $J$  gives the value of  $B_0'(P) - B_0'' = -0.00849 \text{ cm}^{-1}$ . The  $P$  branch can be traced close enough to  $\nu_0$ , whose position is given by the  $Q$  head, to fix the  $J$  numbering of the lines. The intercept of  $P(J) - P(J-1)$  at  $J=0$  gives  $B_0'(P) = 0.367 \text{ cm}^{-1}$  and  $B_0'' = 0.378 \text{ cm}^{-1}$ , in poor agreement with the

more exact value of the difference of the  $B$  values given above, but still agreeing within the limits of the experimental error attending this determination. Within the limits of experimental error, then, it may be concluded that all three transitions have the same lower state. Since the  $R$  branch has not been obtained for this band it is not possible to check this conclusion by obtaining the  $\Delta_2F$ 's and comparing them with those of the 5060A  ${}^1\Sigma \rightarrow {}^1\Sigma$  transition.

### B System

Enough of the  $P$  and  $R$  lines of the 5060A (1 $\rightarrow$ 1) vibrational transition (Table IV) have been found to allow the difference of the  $B$  values to be obtained:  $(B_1' - B_1'') = -0.0084 \text{ cm}^{-1}$ . The  $J$  values are not fixed accurately enough to give the  $B$  values with certainty, but the quantities  $B_1' = 0.3650$  and  $B_1'' = 0.3734 \text{ cm}^{-1}$  are probably correct.

The rotational isotope effect in the  $P$  branch was calculated from the equation  $\Delta P_i(J) = (1 - \rho^2)(B_0' - B_0'')J(J+1) - 2JB_0'$ , where  $\rho^2 = \mu/\mu_i = 0.99287$ , and was found to check very well the experimentally measured isotope splitting within the limits of experimental error of determination of the  $B$ 's.  $\mu$  and  $\mu_i$  are the reduced masses  $(m_1 - m_2)/m_1m_2$  of the molecules  $\text{Cu}^{63}\text{F}^{19}$  and  $\text{Cu}^{65}\text{F}^{19}$ , respectively.

### ACKNOWLEDGMENTS

The author expresses deepest appreciation to Professor R. S. Mulliken whose keen interest in the progress of this problem and whose many helpful suggestions greatly speeded the progress of the work. Grateful acknowledgment is also made to Dr. S. Mrozowski for his unflinching enthusiasm and generous advice.



2551.092Å

2468.878Å

FIG. 1. The group of lines around 2500Å of the  ${}^2\Pi \rightarrow {}^2\Sigma$  system of  $\text{HF}^+$ .



FIG. 2. An enlargement of the  $(0'-0)$  and  $(1-1)$  bands of the  ${}^1\Sigma \rightarrow {}^1\Sigma$  system at 5060 Å.



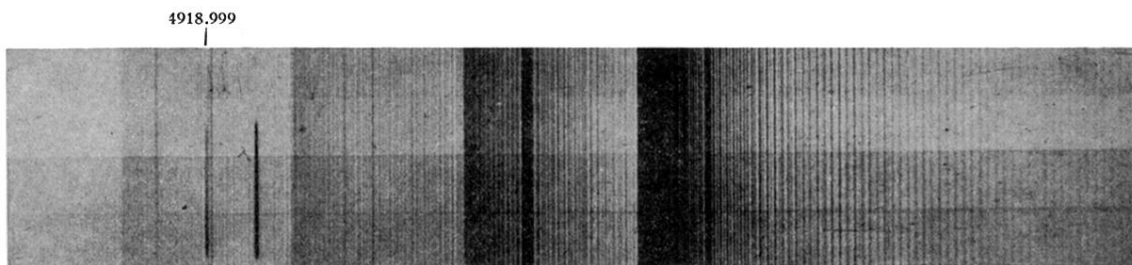


Fig. 3. An enlargement of the *C* system ( ${}^1\Pi \rightarrow {}^1\Sigma$ ) at 4920 Å.

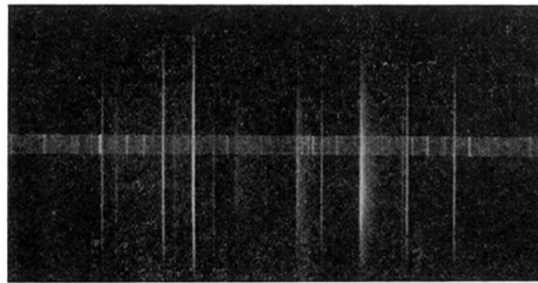


FIG. 4. The  $A$  system of CuF at 5690Å of the type  ${}^1\Pi \rightarrow {}^1\Sigma$ .